Hybrid Concatenated Codes with Asymptotically Good Distance Growth

Christian Koller*, Alexandre Graell i Amat†, Jörg Kliewer‡, Francesca Vatta§, and Daniel J. Costello, Jr.*

*Department of Electrical Engineering, University of Notre Dame, Notre Dame, IN 46556, USA
Email: {dcostel1, ckoller}@nd.edu

† Electronics Department, IT/Telecom Bretagne, 29238 Brest, France
Email: alexandre.graell@telecom-bretagne.eu

‡Klipsch School of Electrical and Computer Engineering, New Mexico State University, Las Cruces, NM 88003, USA
Email: jkliewer@nmsu.edu

§DEEI, Università di Trieste, I-34127 Trieste, Italy
Email: vatta@units.it

***Abstract*—Turbo Codes and multiple parallel concatenated codes (MPCCs) yield performance very close to the Shannon limit. However, they are not asymptotically good, in the sense of having the minimum distance grow linearly with the length of the code. At the other extreme, multiple serially concatenated codes (MSCCs), for example very simple repeat-accumulate-accumulate codes, have proven to be asymptotically good, but they suffer from a convergence threshold far from capacity.**

In this paper, we investigate hybrid concatenated coding structures consisting of an outer MPCC with very simple memory-1 component encoders serially concatenated with an inner accumulator. We show that such structures exhibit linear distance growth with block length and that they have better thresholds than MSCCs. The results indicate a fundamental tradeoff between minimum distance growth and convergence threshold in turbo-like codes.

I. Introduction

The invention of Turbo Codes by Berrou et al. in 1993 [1] revolutionized the field of channel coding. Concatenated coding schemes, consisting of relatively simple component codes separated by interleavers, became a research focus and many related schemes were subsequently proposed. Concatenated coding schemes can be divided into two main categories, parallel concatenated codes (PCCs) and serially concatenated codes (SCCs), introduced by Benedetto et al. in 1998 [2]. PCCs can perform close to channel capacity, but their minimum distance might not be sufficient to yield very low bit error rates at moderate to high signal-to-noise ratios (SNRs), leading to the so-called error floor problem. The minimum distance of a PCC can be improved by adding more branches of parallel concatenation, creating a multiple parallel concatenated code (MPCC), but upper bounds on the minimum distance of MPCCs show that these codes cannot be asymptotically good in the sense that their minimum distance grows linearly with block length [3].

This work was partly supported by NSF grants CCR02-05310 and CCF05-15012, NASA grant NNX07AK536, German Research Foundation (DFG) grant KL 1080/3-1, the University of Notre Dame Faculty Research Program, and the Marie Curie Intra-European Fellowship within the 6th European Community Framework Programme.

SCCs in general exhibit lower error floors than PCCs, due to their better minimum distance, but they usually converge further away from channel capacity. While the minimum distance of single-serially concatenated codes (SSCCs) also cannot grow linearly with block length [3], [4], multiple serially concatenated codes (MSCCs) can be asymptotically good. This has been shown for repeat-multiple accumulate codes in [5] and [6], where the method in [6] allows the exact calculation of the growth rate coefficient. However, the convergence properties of SCCs with three or more concatenation stages are far from capacity. While every additional serially concatenated encoder increases the minimum distance of the code, the iterative decoding behavior degrades, making coding schemes with more than three serially concatenated component codes impractical.

The main goal of this paper is to identify code ensembles that exhibit a minimum distance that grows linearly with block length but still maintains good convergence properties. This motivates us to look at the distance growth and convergence properties of hybrid concatenated codes (HCCs). HCCs offer more freedom in code design and opportunities to combine the advantages of parallel and serially concatenated systems. Several different hybrid concatenated structures have been proposed in the literature, e.g., [7], [8], [9]. Also, in [10], an inner code was used to improve the distance properties of an outer turbo code.

In this paper we show that the minimum distance of HCCs that consist of an outer MPCC serially concatenated with an inner accumulator grows linearly with block length and that these hybrid concatenated schemes can have better iterative decoding thresholds than MSCCs. As a benchmark, we will compare these HCCs to the repeat-accumulate-accumulate MSCC.

II. Encoder Structure and Weight Enumerators

The hybrid code ensembles considered in this paper consist of a MPCC outer code with 4 parallel branches, serially concatenated with a (possibly punctured) accumulator. Figure

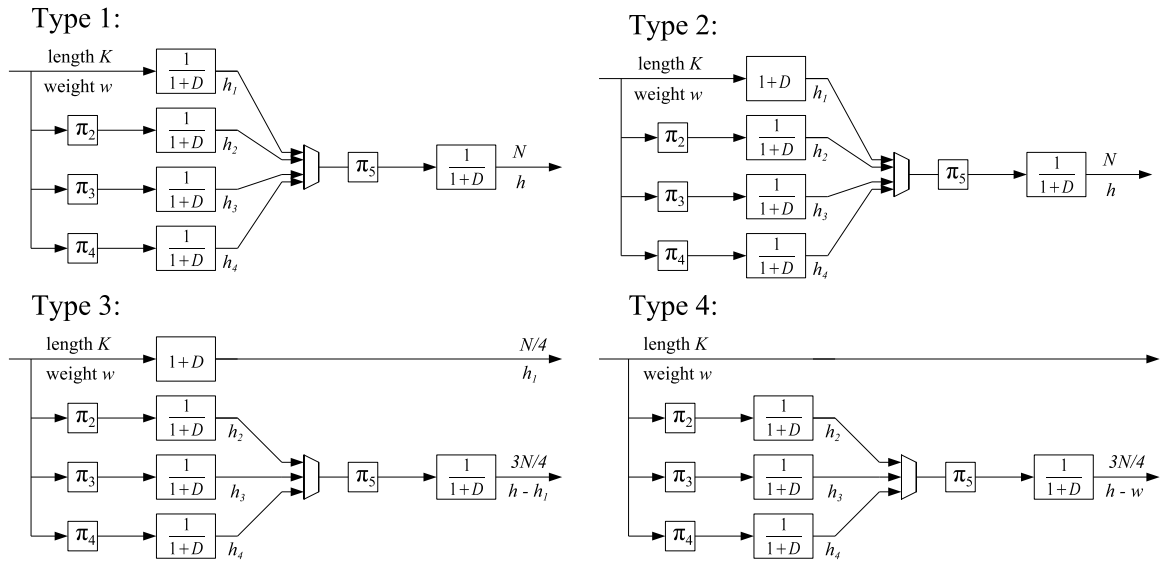

Fig. 1. Encoder structure for hybrid concatenated codes. A possible puncturing of the inner accumulator is not shown here.

1 depicts four different rate $R = 1/4$ encoders considered. In the type 1 and 2 codes, all the code bits from the outer MPCC enter the inner accumulator, while in the type 3 and 4 codes only three of the four parallel branches enter the inner accumulator. The type 1 HCC is, in both its asymptotic distance growth and convergence threshold, identical to the rate $R = 1/4$ repeat by 4-accumulate-accumulate ($\mathrm{R}^4\mathrm{AA}$) code. For a fixed block length and random interleavers the distance spectrum is different, however. The outer MPCC of the type 2 HCC, first introduced in [11], is known to have better convergence behavior than the outer MPCC of the type 1 HCC, due to the presence of a feedforward $(1 + D)$ branch. Higher rates can be obtained by puncturing the outer MPCC or the inner accumulator. In this paper, we consider only random puncturing of the inner accumulator, since otherwise we cannot guarantee the linear distance growth property [6]. For the punctured inner accumulator, we define the puncturing permeability rate δ, $0 \leq \delta \leq 1$, as the fraction of bits that survive after puncturing. Let R' be the rate of the unpunctured code ensemble. Then the rate of the punctured code is given by $R = R'/\delta$ for the type 1 and type 2 codes and by $R = 1/(\delta(R'^{-1} - 1) + 1)$ for the type 3 and type 4 codes. For example, for type 3 and type 4 codes with permeability rate $\delta = 2/3$, the overall code rate is $R = 1/3$.

To analyze the weight spectrum of HCCs, we adopt the uniform interleaver approach from [2] and [12]. Let the HCC consist of L component convolutional encoders and $L - 1$ interleavers. After termination, the lth component code is an (N_l, K_l) linear block code and every encoder $\mathcal{C}_l$, except $\mathcal{C}_1$ which is directly connected to the input, is preceded by a uniform random interleaver π_l. The interleaver π_l of length K_l maps an input of weight w_l into all of its $\binom{K_l}{w_l}$ possible permutations with equal probability. Without loss of generality, we assume that code $\mathcal{C}_L$ is always connected to the channel. Finally, we take the set $\{1, 2, \cdots, L - 1\}$ and separate it into two disjoint sets: the set $\mathcal{S}_O$ of all indices l for which component encoder $\mathcal{C}_l$ is connected to the channel and the set $\bar{\mathcal{S}_O}$, its complement.

Let $A^{\mathcal{C}}_{w,h}$ denote the Input-Output Weight Enumerating Function (IOWEF) of a code $\mathcal{C}$, the number of codewords of length N in $\mathcal{C}$ with input weight w and output weight h. The average IOWEF of an HCC is then given by

$$\begin{aligned}\bar{A}^{\mathcal{C}_{hyb}}_{w,h} &= \sum_{h_1=1}^{N_1} \cdots \sum_{h_{L-1}=1}^{N_{L-1}} A^{\mathcal{C}_1}_{w,h_1} \frac{A^{\mathcal{C}_L}_{w_L, h-\sum_{l\in\mathcal{S}_O} h_l}}{\binom{K_L}{w_L}} \prod_{l=2}^{L-1} \frac{A^{\mathcal{C}_l}_{w_l,h_l}}{\binom{K_l}{w_l}} \\ &= \sum_{h_1=1}^{N_1} \cdots \sum_{h_{L-1}=1}^{N_{L-1}} \bar{A}_{w,h_1,\cdots,h_{L-1},h},\end{aligned} \tag{1}$$

where we call the quantity $\bar{A}_{w,h_1,\cdots,h_{L-1},h}$, with the output weights of each component encoder fixed, the average Conditional Weight Enumerating Function (CWEF).

Likewise, let $\bar{A}^{\mathcal{C}}_h$ denote the average Weight Enumerating Function (WEF) of a code $\mathcal{C}$, the number of codewords with output weight h, i.e.,

$$\bar{A}^{\mathcal{C}}_h = \sum_{w=1}^{K} \bar{A}^{\mathcal{C}}_{w,h}. \tag{2}$$

Since we are using very simple rate-1 component encoders with memory one, their IOWEFs can be given in closed form as [12]

$$A^{\frac{1}{1+D}}_{w,h} = A^{1+D}_{h,w} = \binom{N-h}{\lfloor w/2 \rfloor} \binom{h-1}{\lceil w/2 \rceil - 1}. \tag{3}$$

Finally, using the average IOWEF in (1) along with the union bound, the bit-error rate (BER) of an (N, K) HCC can be upper bounded by

$$P_b \leq \frac{1}{2} \sum_{h=1}^{N} \sum_{w=1}^{K} \frac{w}{K} \bar{A}^{\mathcal{C}_{hyb}}_{w,h} \operatorname{erfc}\left(\sqrt{\frac{hRE_b}{N_0}}\right), \tag{4}$$

where E_b/N_0 is the SNR of an additive white Gaussian noise (AWGN) channel, and we have assumed BPSK modulation.

III. Asymptotic Minimum Distance Analysis

Following [13], we define the asymptotic spectral shape as

$$r(\rho) = \lim_{N\to\infty} \frac{\log \bar{A}^{\mathcal{C}}_{\rho N}}{N}, \tag{5}$$

where $\rho = \frac{h}{N}$ is the normalized codeword weight. When $r(\rho) < 0$, the average number of codewords with normalized weight ρ goes to zero as N gets large.

Now recall Stirling's approximation for binomial coefficients

$$\binom{n}{k} \overset{n\to\infty}{\longrightarrow} e^{n\mathbb{H}(k/n)}, \tag{6}$$

where $\mathbb{H}(\cdot)$ denotes the binary entropy function with the natural logarithm. Then we can write the CWEF of an HCC as

$$\bar{A}_{w,h_1,\cdots,h} = \exp\left\{f(\alpha,\beta_1,\cdots,\beta_{L-1},\rho)\,N + o(N)\right\}, \tag{7}$$

where $\alpha = \frac{w}{K}$, is the normalized input weight, $\beta_l = \frac{h_l}{N_l}$ is the normalized output weight of the component encoders, and the function $f(\cdots)$ is obtained by applying Stirling's approximation to the binomial coefficients in $\bar{A}_{w,h_1,\cdots,h_{L-1},h}$. Using (7), the spectral shape function can now be written as

$$r(\rho) = \sup_{0<\alpha,\beta_1,\cdots,\beta_{L-1}\le 1} f(\alpha,\beta_1,\cdots,\beta_{L-1},\rho), \tag{8}$$

so if the function $f(\cdots)$ is strictly negative for all possible paremeters $0 < \alpha,\beta_1,\cdots,\beta_{L-1} \le 1$, almost all codes in the ensemble do not have a codeword of normalized weight ρ. Further, if $f(\cdots)$ is stricly negative for all ρ, $0 < \rho < \rho_0$, and has a positive supremum for $\rho > \rho_0$, it follows that almost all codes in the ensemble have a minimum distance of at least $\rho_0 N$ as the block length N tends to infinity, i.e., ρ_0 is the asymptotic minimum distance growth rate of the ensemble. To analyze a particular code ensemble, we must solve the resulting optimization problem.

Example 1. *Type 1 HCC:*

To simplify the notation, we denote the input weight of the inner serial accumulator as $h_p = h_1 + h_2 + h_3 + h_4$ and its normalized weight as $\beta_p = \frac{h_p}{N}$. Since the inner accumulator is the only component encoder connected to the channel, the set $\mathcal{S}_O$ is empty, and from (1) the CWEF of the type 1 HCC can be written as

$$\bar{A}^{\mathcal{C}_{type1}}_{w,h_1,\ldots,h_4,h} = \frac{\prod_{l=1}^{4}\binom{K-h_l}{\lfloor w/2\rfloor}\binom{h_l-1}{\lceil w/2\rceil-1}}{\binom{K}{w}^3}\cdot\frac{\binom{N-h}{\lfloor h_p/2\rfloor}\binom{h-1}{\lceil h_p/2\rceil-1}}{\binom{N}{h_p}}, \tag{9}$$

which, using (6), results in the function

$$\begin{aligned} f(\alpha,\beta_1,\cdots,\beta_4,\rho) = {} & \frac{1}{4}\sum_{l=1}^{4}(1-\beta_l)\mathbb{H}\left(\frac{\alpha}{2(1-\beta_l)}\right) + \\ & \frac{1}{4}\sum_{l=1}^{4}\beta_l\mathbb{H}\left(\frac{\alpha}{2\beta_l}\right) + (1-\rho)\mathbb{H}\left(\frac{\beta_p}{2(1-\rho)}\right) + \\ & \rho\mathbb{H}\left(\frac{\beta_p}{2\rho}\right) - \frac{3}{4}\mathbb{H}(\alpha) - \mathbb{H}(\beta_p). \end{aligned} \tag{10}$$

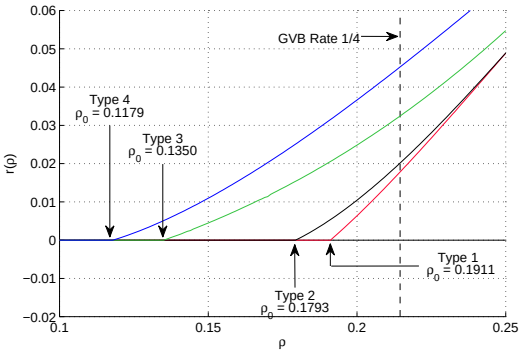

Fig. 2. Asymptotic spectral shape for the rate $R = 1/4$ HCCs in Fig. 1.

The numerical evaluation of (10) and (8) is shown in Figure 2. Although the supremum of (10) is zero for $\rho < \rho_0 = 0.1911$, the supremum is only achieved for $\alpha,\beta_1,\cdots\beta_4 = 0$ and for $0 < \alpha,\beta_1,\cdots,\beta_4 \le 1$ the function $f(\cdots)$ is strictly negative. Thus $\rho_0 = 0.1911$ is the asymptotic minimum distance growth rate of the ensemble.

The function $f(\cdots)$ achieves its maximum when the parallel concatenated encoders contribute equally to the output weight of the outer MPCC, namely when $\beta_1 = \beta_2 = \beta_3 = \beta_4$. Thus we can substitute β_p for β_i and (10) becomes exactly equal to the expression for the double serially concatenated R^{4}AA code.

Example 2. *Type 4 HCC:*

The type 4 HCC is systematic and again we use (1) to obtain its average IOWEF. Since the systematic branch (the first encoder $\mathcal{C}_1$) just performs identity mapping, its IOWEF is given by $A^{\mathcal{C}_1}_{w,w} = \binom{K}{w}$ and zero for all other output weights. Here the systematic branch ($\mathcal{C}_1$) as well as the inner accumulator ($\mathcal{C}_5$) are connected to the channel, so $\mathcal{S}_O = \{1\}$. Again, we denote the input weight of the inner serial accumulator as $h_p = h_2 + h_3 + h_4$ and its normalized weight as $\beta_p = \frac{h_p}{3N/4}$. This results in the following average weight enumerator for the type 4 HCC:

$$\bar{A}^{\mathcal{C}_{type4}}_{w,h_2,\cdots,h} = \frac{\prod_{l=2}^{4}\binom{K-h_l}{\lfloor w/2\rfloor}\binom{h_l-1}{\lceil w/2\rceil-1}}{\binom{K}{w}^2}\cdot\frac{\binom{3N/4-h+w}{\lfloor h_p/2\rfloor}\binom{h-w-1}{\lceil h_p/2\rceil-1}}{\binom{3N/4}{h_p}}, \tag{11}$$

which gives the function

$$\begin{aligned} f(\alpha,\beta_2,\cdots,\rho) = {} & \frac{1}{4}\sum_{l=2}^{4}(1-\beta_l)\mathbb{H}\left(\frac{\alpha}{2(1-\beta_l)}\right) + \\ & \frac{1}{4}\sum_{l=2}^{4}\beta_l\mathbb{H}\left(\frac{\alpha}{2\beta_l}\right) + \left(\frac{3-\alpha}{4}-\rho\right)\mathbb{H}\left(\frac{3\beta_p}{2(3-4\rho+\alpha)}\right) + \\ & \left(\rho-\frac{\alpha}{4}\right)\mathbb{H}\left(\frac{3\beta_p}{2(4\rho-\alpha)}\right) - \frac{1}{2}\mathbb{H}(\alpha) - \frac{3}{4}\mathbb{H}(\beta_p). \end{aligned} \tag{12}$$

Figure 2 shows the spectral shape function for the four different HCCs, along with the Gilbert-Varshamov bound (GVB) for rate $R = 1/4$, the asymptotic distance growth rate of the entire ensemble of block codes. The type 1 scheme has the largest distance growth rate coefficient of 0.1911.

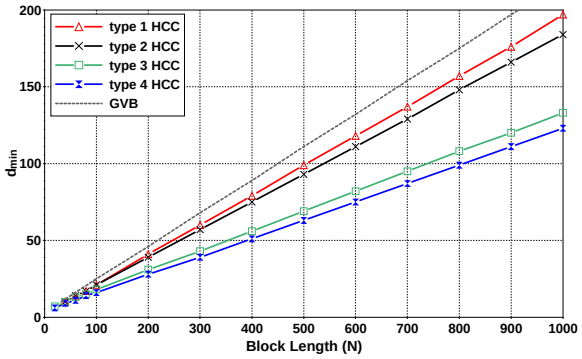

Fig. 3. Lower bound on the minimum distance of the $R = 1/4$ HCCs in Fig. 1.

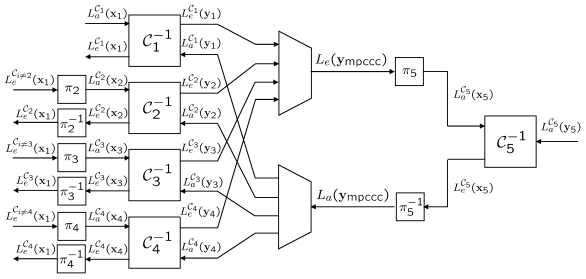

Fig. 4. Decoder for type 1 HCC of Fig. 1.

Replacing one of the parallel concatenated accumulators by its feedforward inverse (type 2) decreases the distance growth rate coefficient to 0.1793. When only three branches enter the inner serially concatenated accumulator and the output of the $(1 + D)$ branch is sent straight through to the channel (type 3), the distance growth rate coefficient reduces to 0.1350, and for the systematic type 4 scheme we obtain a distance growth rate coefficient of 0.1179.

IV. Finite Length Minimum Distance Analysis

The average WEF $\bar{A}_h^{\mathcal{C}_{hyb}}$ can also be used to analyze the finite length minimum distance properties of an HCC ensemble. Given $\bar{A}_h^{\mathcal{C}_{hyb}}$, the probability that a code chosen randomly from the ensemble has minimum distance $d_{\min} < d$ is upper bounded by [5]

$$\Pr(d_{\min} < d) \leq (\bar{A}_0^{\mathcal{C}_{hyb}} - 1) + \sum_{h=1}^{d-1} \bar{A}_h^{\mathcal{C}_{hyb}}. \qquad (13)$$

Equation (13) can now be used to obtain results on the achievable minimum distances of finite length HCCs. In Fig. 3, we show the bound of (13), where we set $\Pr(d_{\min} < d) = 1/2$, for the $R = 1/4$ HCCs in Fig. 1 and codeword lengths up to 1000. By setting $\Pr(d_{\min} < d) = 1/2$, we expect that at least half of the codes in the ensemble have a minimum distance of at least $d_{\min}$. The finite length GVB is also plotted for reference. The results are in agreement with the asymptotic analysis of the previous section. Examining Fig. 3, we observe that the best distance growth rate is obtained for the type 1 HCC, and among the four code ensembles considered, the type 4 HCC exhibits the poorest growth rate. We also note that the growth rate for the type 1 HCC is identical to that of the R^{4}AA code. Due to their larger minimum distances, type 1 and type 2 code ensembles are expected to show lower error floors than type 3 and type 4 HCCs, although they might behave differently in the low SNR regime. The low SNR convergence behavior of these HCCs is analyzed in the next section.

V. Convergence Analysis

A primary goal of this paper is the design of codes with linear distance growth and good convergence properties. The asymptotic minimum distance and finite length analyses in Sections III and IV, respectively, provide accurate predictions of the performance of HCCs in the so-called error floor (moderate to high SNR) region of the bit error rate (BER) curve. However, they convey no information about code performance in the waterfall (low SNR) region. Instead, extrinsic information transfer (EXIT) charts [14] can be used to predict the convergence behavior of iterative decoding for turbo and turbo-like codes, assuming an infinite interleaver size.

Let $\mathbf{x}$ and $\mathbf{y}$ be the sequences of information and coded bits, respectively, of a code $\mathcal{C}$. Also let x_i and y_i be the i-th elements in $\mathbf{x}$ and $\mathbf{y}$. We denote by $L_a^{\mathcal{C}}(x_i)$ and $L_a^{\mathcal{C}}(y_i)$ the a priori values (log-likelihood ratios) of the information bits and coded bits of $\mathcal{C}$, respectively. The soft-input soft-output (SISO) decoder for $\mathcal{C}$ computes the extrinsic log-likelihood ratios (LLRs) $L_e^{\mathcal{C}}(x_i)$ and $L_e^{\mathcal{C}}(y_i)$ based on the a priori information and code constraints.

Now let $I_{A(x)}^{\mathcal{C}}$ and $I_{A(y)}^{\mathcal{C}}$ denote the mutual information (MI) of $L_a^{\mathcal{C}}(x_i)$ and $L_a^{\mathcal{C}}(y_i)$, defined as the mutual information between x_i and $L_a^{\mathcal{C}}(x_i)$, $I(x_i; L_a^{\mathcal{C}}(x_i))$ (respectively, y_i and $L_a^{\mathcal{C}}(y_i)$, $I(y_i; L_a^{\mathcal{C}}(y_i))$). The average a priori MI for the elements in $\mathbf{x}$ and $\mathbf{y}$ is defined as:

$$\begin{aligned} I_{A(x)}^{\mathcal{C}} &= \frac{1}{N} \sum_{i=0}^{N-1} I(x_i; L_a^{\mathcal{C}}(x_i)) \\ I_{A(y)}^{\mathcal{C}} &= \frac{1}{N} \sum_{i=0}^{N-1} I(y_i; L_a^{\mathcal{C}}(y_i)). \end{aligned} \qquad (14)$$

In a similar way, we can define the average extrinsic MIs $I_{E(x)}^{\mathcal{C}}$ and $I_{E(y)}^{\mathcal{C}}$ for the extrinsic LLRs. The input-output behavior of a SISO decoder for code $\mathcal{C}$ is then completely characterized by two EXIT functions, T_x and T_y, which specify the evolution of the extrinsic MIs as a function of the a priori MIs:

$$\begin{aligned} I_{E(x)}^{\mathcal{C}} &= T_x(I_{A(x)}^{\mathcal{C}}, I_{A(y)}^{\mathcal{C}}) \\ I_{E(y)}^{\mathcal{C}} &= T_y(I_{A(x)}^{\mathcal{C}}, I_{A(y)}^{\mathcal{C}}). \end{aligned} \qquad (15)$$

In practice, these functions can be obtained by Monte Carlo simulation for all values $0 \leq I_{A(x)}^{\mathcal{C}} \leq 1$ and $0 \leq I_{A(y)}^{\mathcal{C}} \leq 1$ by modeling the a priori information as Gaussian distributed.

In a coding scheme with L component encoders, decoding proceeds by alternating between the L SISO decoders. The evolution of the extrinsic MI can then be tracked in a multi-dimensional EXIT chart [15], which can be used to predict the convergence threshold. Unfortunately, such a multi-dimensional EXIT chart is hard to visualize. To generate EXIT charts that are easy to deal with, the EXIT functions of the $L - 1$ component encoders of the outer MPCCCs in Fig. 1 can be combined to obtain the EXIT function of the MPCCC.

Thus, the behavior of the HCC structures considered in this paper can be determined by using a two-dimensional EXIT chart, displaying in a single figure the EXIT functions of the outer MPCCC and the inner accumulator. To compute the EXIT function of the MPCCC we follow the approach suggested in [16]. As an example, consider the type 1 HCC in Fig. 1. The corresponding decoder is depicted in Fig. 4. Following the above definitions, let $L_a^{\mathcal{C}_l}(\mathbf{x}_i)$ and $L_a^{\mathcal{C}_l}(\mathbf{y}_i)$ ($L_e^{\mathcal{C}_l}(\mathbf{x}_i)$ and $L_e^{\mathcal{C}_l}(\mathbf{y}_i)$) denote the a priori information (extrinsic information) for $\mathbf{x}_i$ and $\mathbf{y}_i$ for code $\mathcal{C}_l$. Similarly, let $I_{A(\mathbf{x}_i)}^{\mathcal{C}_l}$, $I_{A(\mathbf{y}_i)}^{\mathcal{C}_l}$ ($I_{E(\mathbf{x}_i)}^{\mathcal{C}_l}$, $I_{E(\mathbf{y}_i)}^{\mathcal{C}_l}$) denote the corresponding MIs. The EXIT functions for the lth component code ($l = \{1, \ldots, 4\}$) can then be expressed as

$$I_{E(\mathbf{x}_l)}^{\mathcal{C}_l} = T_x^{\mathcal{C}_l}\left(J\left(\sqrt{\sum_{i=1, i\neq l}^{L-1} J^{-1}\left(I_{E(\mathbf{x}_i)}^{\mathcal{C}_i}\right)^2}\right), I_{A(\mathbf{y}_l)}^{\mathcal{C}_l}\right)$$
$$I_{E(\mathbf{y}_l)}^{\mathcal{C}_l} = T_y^{\mathcal{C}_l}\left(J\left(\sqrt{\sum_{i=1, i\neq l}^{L-1} J^{-1}\left(I_{E(\mathbf{x}_i)}^{\mathcal{C}_i}\right)^2}\right), I_{A(\mathbf{y}_l)}^{\mathcal{C}_l}\right), \quad (16)$$

where closed form approximations for the function J and its inverse J^{-1} can be found in [14], [16]. Note that, for the type 1 HCC, the four EXIT functions $I_{E(\mathbf{x}_l)}^{\mathcal{C}_l}$ are identical and $I_{A(\mathbf{y}_l)}^{\mathcal{C}_l} = I_{E(\mathbf{x}_5)}^{\mathcal{C}_5}$.

The EXIT function of the MPCCC, $I_{E(\mathbf{y}_{\text{mpccc}})}^{\mathcal{C}_{mpccc}}$, can be computed for all values $0 \leq I_{E(\mathbf{x}_5)}^{\mathcal{C}_5} \leq 1$ by activating all $L-1$ decoders of the MPCCC until $I_{E(\mathbf{x}_l)}^{\mathcal{C}_l}$ and $I_{E(\mathbf{y}_l)}^{\mathcal{C}_l}$ have converged to a fixed value. Then $I_{E(\mathbf{y}_{\text{mpccc}})}^{\mathcal{C}_{mpccc}}$ is just equal to $I_{E(\mathbf{y}_l)}^{\mathcal{C}_l}$. Finally, the convergence behavior of the HCCs considered here can be tracked by displaying in a single plot the EXIT functions $I_{E(\mathbf{y}_{\text{mpccc}})}^{\mathcal{C}_{mpccc}} = T(I_{E(\mathbf{x}_5)}^{\mathcal{C}_5})$ and $I_{E(\mathbf{x}_5)}^{\mathcal{C}_5} = T(I_{E(\mathbf{y}_{\text{mpccc}})}^{\mathcal{C}_{mpccc}}, \delta J(\sqrt{8RE_b/N_0}))$, where δ represents the permeability rate if puncturing is employed. A similar procedure as the one described above can be applied for the type 3 and type 4 HCCs. In this case, the EXIT function for the outer MPCCC also depends on the SNR. For the type 2 HCC, the computation of $I_{E(\mathbf{y}_{\text{mpccc}})}^{\mathcal{C}_{mpccc}}$ is a bit more complex, since the EXIT function of the first encoder in the outer MPCCC is different.

The resulting EXIT charts are shown in Fig. 5 for type 1 and type 4 HCCs and rate $1/4$. The dashed curves are the EXIT functions for the inner and outer codes of the type 1 HCC for $E_b/N_0 = 2.24$ dB, while the solid curves are the EXIT functions of the type 4 HCC for $E_b/N_0 = 1.03$ dB. A vertical step between the lower curves and the upper curves represents a single activation of the inner decoder, while a horizontal step between the upper curves and the lower curves represents an unspecified number of activations of all the component decoders of the MPCCC until nothing more can be gained. We observe that the type 4 HCC converges significantly earlier (1.21 dB) than the type 1 HCC, thanks to the systematic branch. We also note that the EXIT chart for the type 1 HCC is identical to that of the R^{4}AA code, where

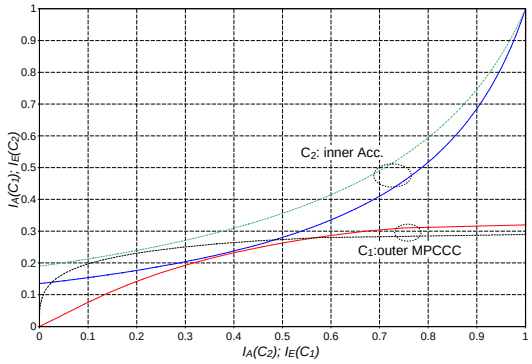

Fig. 5. EXIT charts of type 1 HCC (dashed curves) for $E_b/N_0 = 2.24$ dB and of type 4 HCC (solid curves) for $E_b/N_0 = 1.03$ dB.

TABLE I
DISTANCE GROWTH RATE COEFFICIENT ρ_0 VERSUS CONVERGENCE THRESHOLD FOR DIFFERENT RATE 1/4 AND PUNCTURED RATE 1/3 HCCS.

	rate 1/4		rate 1/3	
Code	ρ_0	threshold	ρ_0	threshold
Type 1	0.1911	2.24 dB	0.1669	2.85 dB
Type 2	0.1793	2.05 dB	0.1650	2.60 dB
Type 3	0.1350	1.30 dB	0.1172	1.94 dB
Type 4	0.1179	1.03 dB	0.1057	1.40 dB
RAA	0.1911	2.24 dB	0.1323	1.68 dB

the EXIT function for $\mathcal{C}_1$ in the figure corresponds now to the EXIT function of the R^{4}A outer code.

From the minimum distance and EXIT chart analyses, it is seen that the hierarchy of the codes in terms of convergence threshold is opposite to their hierarchy in terms of distance growth, i.e., the best schemes in terms of distance growth are the worst ones in terms of convergence, and vice versa. In Table I we give the asymptotic distance growth rate coefficient ρ_0 and the convergence threshold for the four HCCs in Fig. 1 for rates $R = 1/4$ and 1/3[1], where the rate $R = 1/3$ results were obtained by modifying the analyses of Sections III and IV to account for random puncturing of the inner accumulator. The results indicate the presence of a fundamental tradeoff between distance growth and convergence properties. This tradeoff has been also often observed in finite length analyses of many kinds of concatenated codes: the codes attaining lower error floors are in general those with poorer convergence thresholds.

VI. SIMULATION RESULTS

In Fig. 6 we give BER curves for the rate $R = 1/4$ HCCs of Fig. 1, together with the union bounds on error probability obtained from (4). The information block length is $K = 1024$ bits and random interleavers are assumed. The type 1 and type 2 HCCs exhibit the best performance in the error floor region, but they have poor convergence behavior. Convergence is significantly improved if some bits from the outer code are not encoded by the inner accumulator. As anticipated by the EXIT charts analysis, the best convergence is achieved by the systematic type 4 HCC. On the other hand, this code has the worst error floor behavior, as anticipated by the distance growth rate results of Figs. 2 and 3. In the same figure we show the BER curve and the union bound for the R^{4}AA code.

[1]The RAA results for rate 1/3 are for the true rate 1/3 R^3AA code ensemble, not for the punctured R^4AA code ensemble.

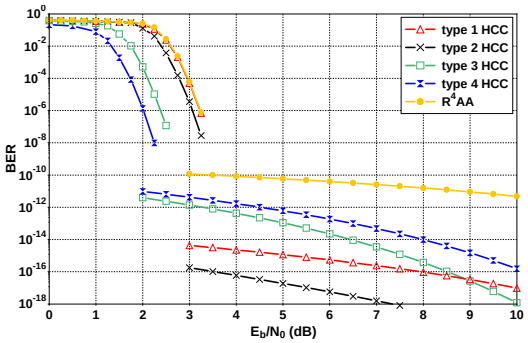

Fig. 6. Bit error probability performance for rate $R = 1/4$ HCCs on an AWGN channel. $K = 1024$ bits.

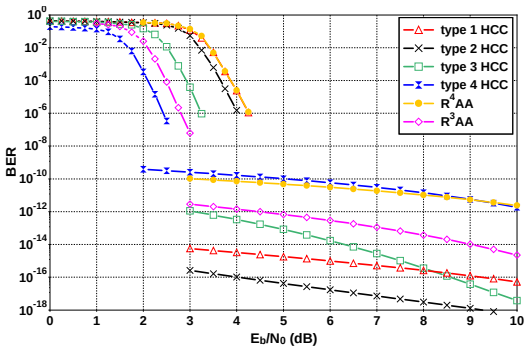

Fig. 7. Bit error probability performance for rate $R = 1/3$ HCCs on an AWGN channel. $K = 1024$ bits.

Note that its performance in the waterfall region is identical to the type 1 HCC, as predicted by the EXIT charts. Finally, in Fig. 7 we give BER curves for punctured rate $R = 1/3$ HCCs, together with their union bounds. The performance of the R^3AA code is also shown. We see that the type 4 HCC is the best code in terms of convergence, where we observe an improvement of ~ 0.4 dB with respect to the R^3AA. On the other hand, the type 4 HCC also has the highest error floor.

The union bounds in Figs. 6 and 7 depend on the entire code ensemble. Therefore, they are dominated by the code with the smallest minimum distance. This explains the error floor disagreement in some cases with respect to the hierarchy noted in Table I. Better agreement is achieved if we compute instead the union bound for an expurgated ensemble [5] (i.e, only for those codes with $d_{\min} \geq d$, where $\Pr(d_{\min} < d) = 0.5$. The expurgated bounds are not plotted in the figures, since they are extremely low. Designed interleavers should be able to attain such very low error floors.

VII. Conclusions

Asymptotically good code ensembles, in the sense that their minimum distance grows linearly with block length, are less prone to error floors than code ensembles without this property. In this paper, we have investigated several rate $R = 1/4$ hybrid concatenated codes with very simple component encoders that have better convergence thresholds than the R^4AA code and are also asymptotically good.

We calculated the asymptotic distance growth rate coefficient of these hybrid concatenates codes using the spectral shape function of the ensemble, presented the corresponding finite length analysis, and determined their iterative decoding thresholds using EXIT charts. Then simulation results were given to support the conclusions of the minimum distance and EXIT chart analyses.

Similar to results of other studies, we observed a trade-off between convergence thresholds and distance growth rates. We conclude that it is not possible to optimize both design criteria at the same time, so that in practice it is necessary to seek a compromise between error floor performance and convergence behavior. Hybrid concatenated codes offer more freedom in designing the encoder structure than multiple serially concatenated codes, and thus it is possible to design code ensembles that offer a better tradeoff between minimum distance growth and iterative decoding convergence behavior.

Finally, we have also observed that the threshold can be further improved by replacing a fraction λ of the output bits of the inner accumulator with the corresponding input bits, thus improving convergence behavior at the expense of distance growth.

References

[1] C. Berrou, A. Glavieux, and P. Thitimajshima, "Near shannon limit error-correcting coding and decoding: Turbo codes," in *Proceedings IEEE International Conference on Communications*, Geneva, May 1993, pp. 1064–1070.

[2] S. Benedetto, D. Divsalar, G. Montorsi, and F. Pollara, "Serial concatenation of interleaved codes: performance analysis, design, and iterative decoding," *IEEE Trans. Inf. Theory*, vol. 44, no. 3, pp. 909–926, May 1998.

[3] N. Kahale and R. Urbanke, "On the minimum distance of parallel and serially concatenated codes," in *Proc. IEEE Int. Symposium on Inform. Theory*, Cambridge, MA, Aug. 1998, p. 31.

[4] L. Bazzi, M. Mahdian, and D. A. Spielman, "The minimum distance of turbo-like codes," Submitted to *IEEE Trans. Inf. Theory*, May 2003.

[5] H. D. Pfister, *On the Capacity of Finite State Channels and the Analysis of Convolutional Accumulate-m Codes*, Ph.D. Thesis, University of California, San Diego, CA, 2003.

[6] J. Kliewer, K. S. Zigangirov, and D. J. Costello, Jr., "New results on the minimum distance of repeat multiple accumulate codes," in *Proc. 45th Annual Allerton Conf. Commun., Control, Computing*, Monticello, IL, Sept. 2007.

[7] D. Divsalar and F. Pollara, "Serial and hybrid concatenated codes with applications," in *Proc. Int. Symp. on Turbo Codes and Related Topics*, Brest, France, Sept. 1997, pp. 80–87.

[8] J. Li, K. R. Narayanan, and C. N. Georghiades, "Product accumulate codes: A class of codes with near-capacity performance and low decoding complexity," *IEEE Trans. Inf. Theory*, vol. 50, pp. 31–46, Jan. 2004.

[9] H. Gonzalez, C. Berrou, and S. Kerouédian, "Serial/parallel turbo codes for low error rates," in *IEEE Military Commun. Conf.*, Paris, France, Sept. 2004, pp. 346–349.

[10] C. Berrou, A. Graell i Amat, Y. Ould-Cheikh-Mouhamedou, C. Douillard, and Y. Saouter, "Improving the distance properties of turbo codes using a third component code: 3d turbo code," in *Proc. IEEE Information Theory Workshop*, Lake Tahoe, Ca, USA, Sept. 2007, pp. 156–161.

[11] P. C. Massey and D. J. Costello, Jr,, "New low-complexity turbo-like codes," in *Proc. IEEE Information Theory Workshop*, Cairns, Australia, Sept. 2001.

[12] D. Divsalar, H. Jin, and R. J. McEliece, "Coding theorems for 'turbo-like' codes," in *Proc. 36th Annual Allerton Conf. Commun., Control, Computing*, Monticello, IL, Sept. 1998, pp. 201–210.

[13] R. G. Gallager, *Low-density parity-check codes*, MIT Press, Cambridge, MA, 1963.

[14] S. ten Brink, "Convergence behavior of iteratively decoded parallel concatenated codes," *IEEE Trans. Comm.*, vol. 49, no. 2, pp. 1727–1737, Oct. 2001.

[15] M. Tüchler, "Convergence prediction for iterative decoding of threefold concatenated systems," in *Proc. IEEE Global Telecommun. Conf.*, Taipeh, Taiwan, Nov. 2002, pp. 1358–1362.

[16] F. Brännström, L. K. Rasmussen, and A. J. Grant, "Convergence analysis and optimal scheduling for multiple concatenated codes," *IEEE Trans. Inf. Theory*, vol. 51, no. 9, pp. 3354–3364, Sept. 2005.